Three-dimensional particle-in-cell method of simulating high power terahertz gyrotrons with planar structure

Chen Zai-Gao(陈再高)[a)b)], Wang Jian-Guo(王建国)[a)b)†], Wang Yue(王 玥)[b)], Qiao Hai-Liang(乔海亮)[b)], Guo Wei-Jie(郭伟杰)[a)], and Zhang Dian-Hui(张殿辉)[b)]

[a)] *School of Electronic and Information Engineering, Xi'an Jiaotong University, Xi'an* 710049, *China*
[b)] *Northwest Institute of Nuclear Technology, P. O. Box* 69-1, *Xi'an* 710024, *China*

(Received 23 October 2013; revised manuscript received 30 November 2013; published online 20 April 2014)

Based on analyzing the large-signal theory of the planar gyrotron, it is suggested that a simplified structure of the device is used for simulating this kind of device, with the working characteristics of the device kept unchanged, i.e., the same as those of the device with the original structure. Thus, the computational burden can be significantly reduced. Using the proposed method, we simulate a planar gyrotron with its simplified parameters by using the UNIPIC-3D code. Numerical results show that the working frequency, output power, and electron efficiency are respectively about 0.813 THz, 14 kW, and 21%.

Keywords: planar gyrotron, terahertz, particle simulation

PACS: 84.40.Fe, 45.10.Db, 52.65.–y **DOI:** 10.1088/1674-1056/23/6/068402

1. Introduction

Recently, high power terahertz waves are pressingly in demand for widespread applications in imaging, radar, high-data-rate communications, plasma heating, medical research, etc.[1–4] These applications require higher-power, more-reliable THz radiation sources. The vacuum electron device has the merit of high power output and relatively compact structure, so many publications concern the vacuum electronic terahertz devices, such as the gyrotron, backward wave oscillator (BWO), surface wave oscillator (SWO), free electron laser, and folded-waveguide traveling wave tube (TWT).[5–10] Among these devices, the gyrotron is one of the most promising sources in the subterahertz band of 0.1 THz–1.0 THz. To improve the electron efficiency and raise the output power of the gyrotron, Ginzburg *et al.*[10] suggested the use of a planar scheme with a sheet electron beam and transverse (with respect to the electron's translation velocity) electromagnetic energy extraction instead of the conventional cylindrical configuration. The main advantage of the new structure is to ensure coherent radiation from a large size planar electron beam. This is due to effective mode selection over the open transverse coordinate and synchronization of radiation from different beam fractions by transverse electromagnetic energy fluxes.

The particle-in-cell (PIC) method is commonly used to design the vacuum electronic devices, but it suffers from the huge computational burden in the simulation of the gyrotron in the terahertz band. First, the simulation of the planar gyrotron should be performed by using the three-dimensional (3D) code. Second, the cell number required to discretize the device is huge. Figure 1 is a typical structure of a planar gyrotron, where the sheet electron beam is injected into the device from its left side, and the terahertz wave is generated by the rotating electrons, whose moving trajectory is shown in Fig. 2. The generated power can be extracted from both of the x directions. The size of the planar gyrotron proposed by Ginzburg *et al.*[10] is about $80\lambda \times 33\lambda \times 13\lambda$, and the spatial increment is very small to resolve the gyroradius of the electron, so the cell number is huge. Third, the time step is very small to satisfy the stability condition, maybe it is 10^{-14} s, so several million time steps are needed to obtain the terahertz signal for several ten nanoseconds.

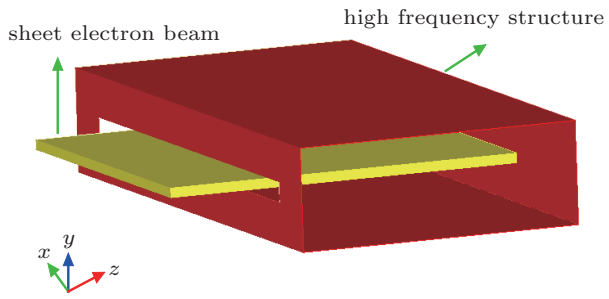


Fig. 1. (color online) Geometric model of planar gyrotron.

To expedite the simulation of the planar gyrotron, we analyze the large-signal theory of the planar gyrotron, and suggest simplifying the structure of the device, meanwhile, keeping the working characteristics of the device unchanged, i.e., maintain their original ones. Thus, the computational burden can be significantly reduced.

The rest of this paper is organized as follows. In Section 2, the simplified model of a planar gyrotron is briefly in-

†Corresponding author. E-mail: wanguiuc@mail.xjtu.edu.cn

© 2014 Chinese Physical Society and IOP Publishing Ltd

troduced. The PIC simulation results of the proposed planar gyrotron are presented in Section 3. Finally some conclusions are drawn from the present study in Section 4.

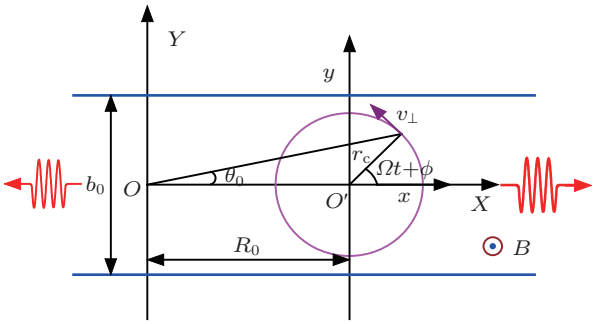


Fig. 2. (color online) Projection of electron orbit in the planar gyrotron.

2. Simplified model of a planar gyrotron

In the planar gyrotron with transverse energy output, the electromagnetic field satisfies[10]

$$\boldsymbol{E} = \boldsymbol{x}\,\mathrm{Re}\left(A\left(x,z,t\right)\sin\left(\pi sy/b_0\right)\exp\left(\mathrm{i}\omega_{c0}t\right)\right), \tag{1}$$

where

$$\omega_{c0} = \pi sc/b_0,$$

b_0 being the space gap between the above and bottom plates, s an integer number, and c the speed of light.

The governing equations are given below for describing the self-consistent interaction between the electron beam and electromagnetic wave,[10]

$$\mathrm{i}\frac{\partial^2 a}{\partial Z^2} + \mathrm{i}\frac{\partial^2 a}{\partial X^2} + \frac{\partial a}{\partial \tau} = F\left(X\right)\frac{G}{\pi}\int_0^{L_Z}\frac{1}{\pi}\int p\,\mathrm{d}\theta, \tag{2a}$$

$$\frac{\partial p}{\partial Z} + \mathrm{i}p\left(-1+|p|^2\right) = -a, \tag{2b}$$

where some dimensionless variables and parameters are

$$\begin{aligned}
&p = \left(p_x + \mathrm{i}p_y\right)e\left(\mathrm{i}\omega_{c0}t\right)/p_{\perp 0},\\
&\tau = \omega_{c0}t\beta_{\perp 0}^4/8\beta_{\|0}^2,\\
&Z = \pi\beta_{\perp 0}^2 z/\beta_{\|0}\lambda,\\
&X = \pi\beta_{\perp 0}^2 x/\beta_{\|0}\lambda,\\
&a = eA/\left(m\omega_{c0}c\beta_{\perp 0}^3\gamma_0\right),\\
&G = 4ej_0\lambda^2\beta_{\|0}/\pi mc^3 b_0\beta_{\perp 0}^6\gamma_0,\\
&\Delta = 2\left(\omega_H - \omega_{c0}\right)/\omega_{c0}\beta_{\perp 0}^2,\\
&F\left(X\right) = 1, X\in\left[0, L_x\right].
\end{aligned}$$

Equation (2a) describes the spatial and temporal distributions of the electric field E_x, and G is the coefficient of the interaction between electron beam and electromagnetic wave. G is inversely proportional to b_0, and the frequency ω_{c0} is determined by b_0 and s. According to the large-signal theory proposed by Ginzburg *et al.*,[10] $P_{\mathrm{total}} = P_{\mathrm{out}} + P_{\mathrm{Ohm}} = 4\eta_\perp GL_x \propto L_x$. Here, we ignore the Ohmic loss of wall, thus, $P_{\mathrm{out}} \propto L_x$. Therefore, by properly reducing b_0, s, and L_x, the computational burden can be significantly reduced and the working property of the device remains unchanged.

Based on the above analysis, we can simplify the structure of the planar gyrotron, which can be numerically simulated by using the 3D fully electromagnetic parallel PIC code UNIPIC-3D. The size of the structure of the planar gyrotron proposed by Ginzburg *et al.*[10] is about 80λ, 33λ, and 13λ in the x, y, and z directions, respectively. To obtain the maximum interaction coefficient, the central line of the electron cyclotron is set to be along that of the maximum amplitude of the electric field. Here, the parameters chosen for simulation of the planar gyrotron are listed in Table 1, the driving voltage is 30 kV, and the guiding magnetic field is set to be 27.6 T.

Table 1. Parameters of a planar gyrotron with transverse output.

Beam voltage/kV	Linear current density/(A/cm)	Pitch factor	Length in x direction/mm	Length in y direction/mm	Length in z direction/mm	Magnetic field strength/T
30	18	1	2.4	0.2	3.8	27.6

3. PIC simulation of the planar gyrotron

The UNIPIC-3D code was developed for 3D simulations of high-power microwave devices,[11] such as the relativistic backward wave oscillator, magnetron, vircator, magnetically insulated line oscillator, etc. The particle boundaries implemented in the UNIPIC-3D code include Gauss's law, field emission, beam injection, space-charge-limited model, secondary electron emission, etc. The open boundaries are truncated by either the Mur-type absorbing boundary condition or the convolutional perfectly matched layer.[12,13] It is the 3D version of the 2.5-dimensional code UNIPIC,[14] which has been used to simulate the high power surface wave oscillator in the subterahertz band.[7,15–19]

We use the UNIPIC-3D code to simulate the planar gyrotron with its structure parameters listed in Table 1. To resolve the gyroradius of the electron, the spatial increment is selected to be 10 μm, so the entire device is discretized into 240×20×380 cells. The time step is chosen to be 10^{-14} s. A sheet electron beam with a length of 1.2 mm and a beam

voltage of 30 kV is injected from the left side of the device as shown in Fig. 1. Typical numerical results are given in Figs. 3–9.

Figure 3 shows the time evolution of the beam current with an average value of about 2.2 A. Figure 4 displays the 3D distribution of the electric field E_x at 4.0 ns. It can be seen that a steady-state mode of the electric field has formed.

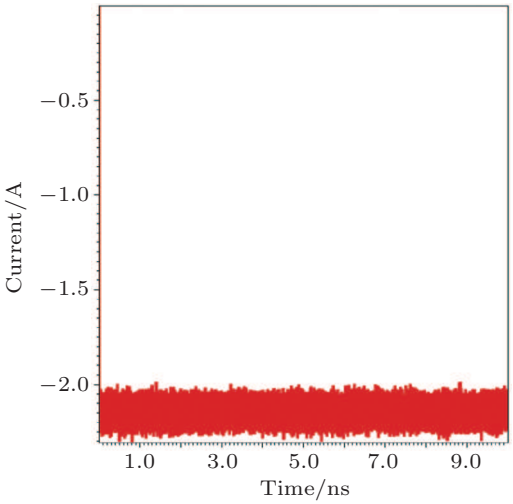


Fig. 3. (color online) Beam current versus time.

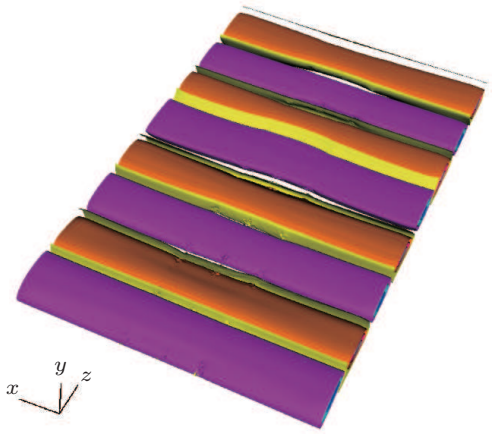


Fig. 4. (color online) 3D distribution of E_x.

Figures 5(a) and 5(b) are the time evolution and the spectrum of the electric field E_x at the output port of the device respectively. Figure 5(b) indicates that the working frequency of the device is about 0.813 THz.

Figure 6 shows the distributions of electron velocity at different times. At 0.5 ns, the electrons are not bunching obviously, so there is no terahertz signal generated, this can also be seen from Fig. 5(a). At 10 ns, the electrons are gyrating and bunching significantly, and the terahertz signal is generated and keeps stable.

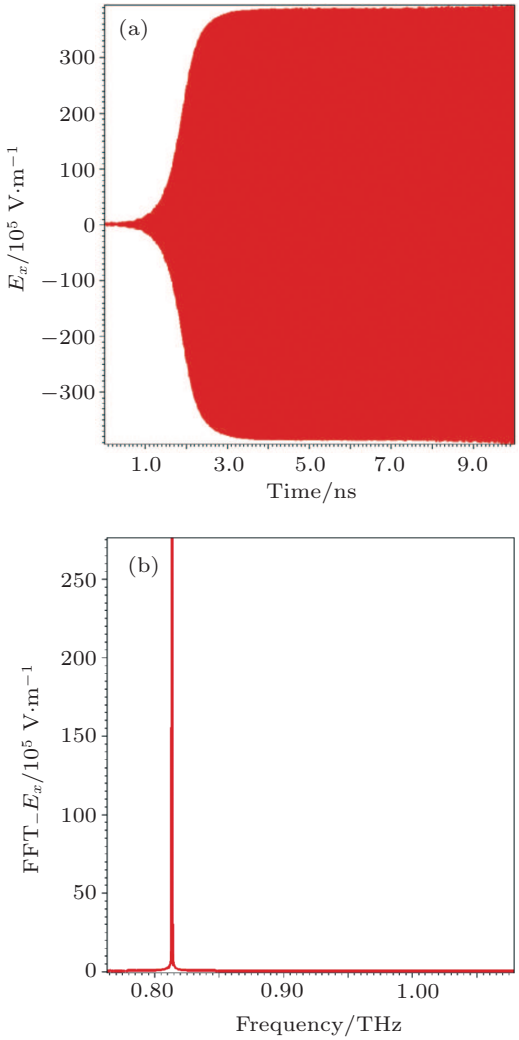


Fig. 5. (color online) (a) E_x versus time and (b) spectrum of output signal (E_x) at output port of the device.

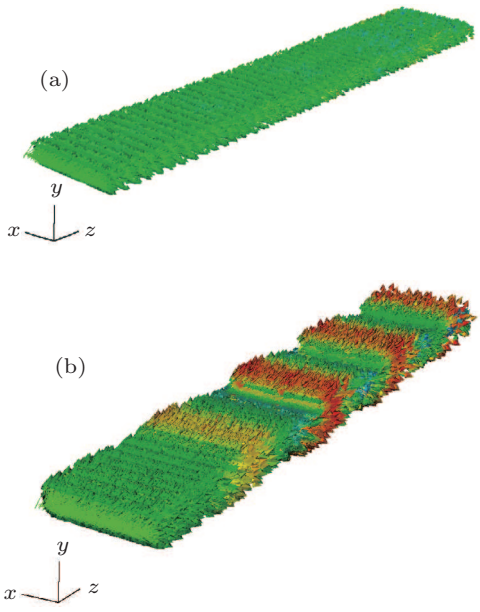


Fig. 6. (color online) Distributions of electron velocity at (a) 0.5 ns and (b) 10 ns.

The simulated output power is presented in Fig. 7, where

figures 7(a) and 7(b) show respectively the output powers from the x and $-x$ directions, their power fluxes are nearly the same in magnitude, but opposite in direction. It can be seen from this figure that the output power is about 14.0 kW, the conversion efficiency of the electron beam to the terahertz wave is about 21%.

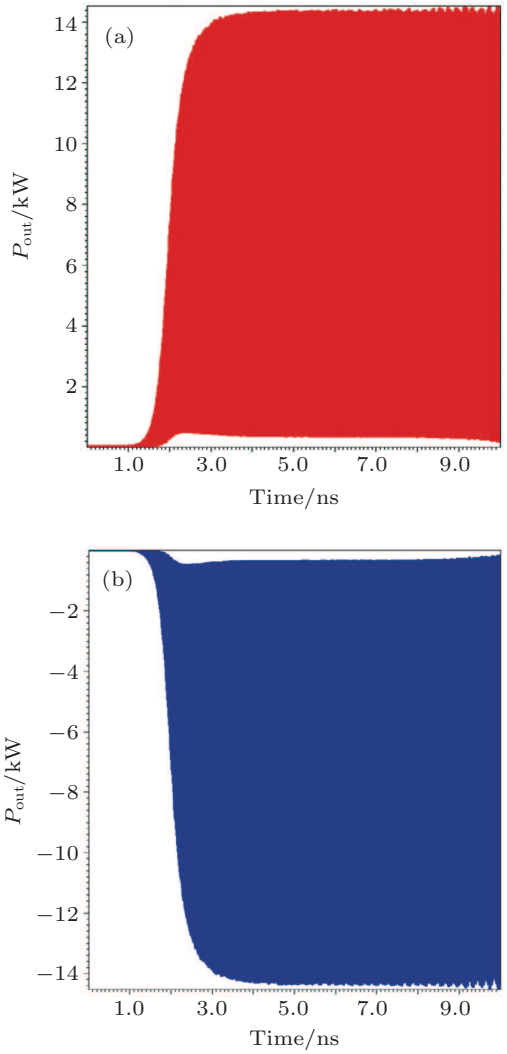


Fig. 7. (color online) Simulated output powers of the planar gyrotron in the (a) x and (b) $-x$ directions.

Now, we recall the example given by Ginzburg *et al.*,[10] where the beam voltage is the same as that used here, and the electron efficiency is about 20% for the electron beam length of 2.4 cm. That is to say, the electron efficiency does not depend on the length of electron beam for a given beam voltage and working frequency.

The working frequency of a gyrotron at the first harmonic of the electron cyclotron frequency is

$$\omega - \frac{eB_0}{m\gamma_0} \approx k_z v_z, \tag{3}$$

where k_z and v_z are the wave vector and velocity in the z direction. If the external magnetic field is changed, the working frequency of a gyrotron is also changed to keep the phase synchronization of the electron with the electromagnetic wave.

Keeping the parameters of the device unchanged and reducing the magnetic field from 27.6 T to 27.4 T, the PIC results are shown in Fig. 8. Figure 8(a) shows the distribution of the electric field E_x at 4.0 ns. It can be seen by comparing this figure with Fig. 4 that the mode is changed from 4 periods at 27.6 T to 3 periods at 27.4 T along the z direction. Figure 8(b) is the output power of the device, it keeps almost unchanged, but the working frequency is reduced to 0.785 THz. Further reducing the magnetic field to 27.2 T, the PIC results are shown in Fig. 9. Figure 9(a) shows the distribution of the electric field E_x at 4.0 ns. It can be seen that the mode is changed from 4 periods at 27.6 T to 2.5 periods at 27.2 T along the z direction. Figure 9(b) is the output power of the device, and it is reduced from about 14 kW at 27.6 T to 12 kW at 27.2 T, so the electron efficiency is reduced to about 18.2% from 21% at 27.6 T correspondingly, meanwhile, the working frequency is reduced to 0.772 THz. Numerical results indicate that the working mode and frequency of the planar gyrotron can be adjusted by changing the external applied magnetic field.

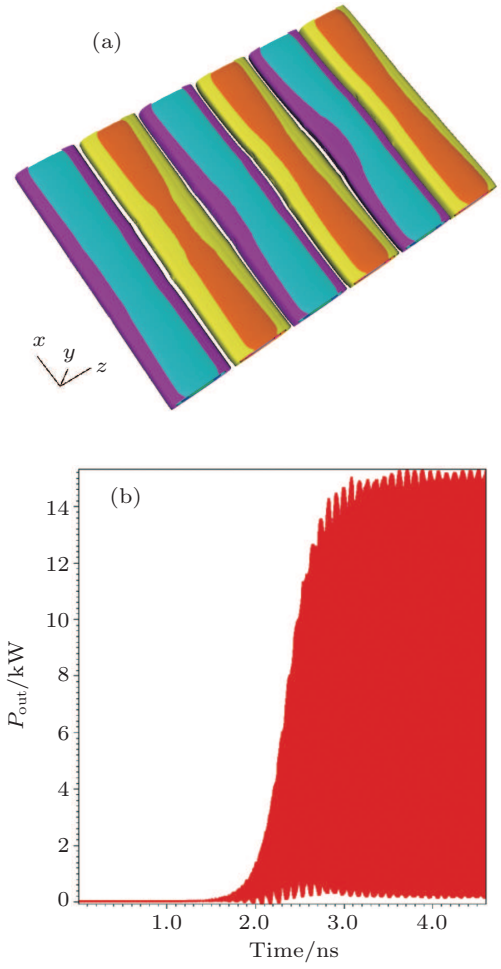


Fig. 8. (color online) Numerical results of the device guided by magnetic field of 27.4 T, showing (a) 3D distribution of E_x at 4.0 ns, and (b) output power versus time.

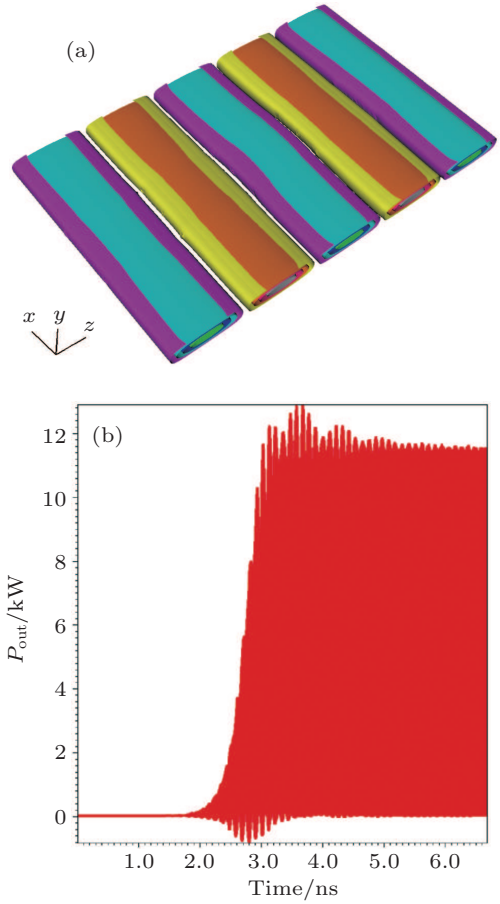


Fig. 9. (color online) Numerical results of the device guided by magnetic field of 27.2 T, showing (a) 3D distribution of E_x at 4.0 ns, and (b) output power versus time.

4. Conclusions

By analyzing the equations describing the self-consistent interaction between electron beam and electromagnetic wave in a planar gyrotron, we propose a method of simplifying the structure of the planar gyrotron to greatly accelerate the PIC simulations of the properties of the device, namely, by properly reducing b_0, s, and L_x, the computational burden can be significantly reduced, meanwhile, the working characteristics of the device (such as the frequency, electron efficiency, and mode, etc.) remain unchanged, i.e., the same as those of the device with the original structure. Therefore, in the design stage of the planar gyrotron, the proposed simplification method can be used.

Using the proposed method, we simulate a planar gyrotron with its parameters listed in Table 1 by using the UNIPIC-3D code. Numerical results show that the working frequency, output power, and electron efficiency are about 0.813 THz, 14 kW, and 21%, respectively.

Corresponding to the working frequency of 0.813 THz, the wavelength is about 0.37 mm, the simplified size of the device is $6.5\lambda \times 0.5\lambda \times 10\lambda$, which is almost 10^3 times smaller than that proposed by Ginzburg *et al.*[10] So the computational speed of such a simplified structure can be at least 10^3 times faster than that of the original structure, and the working characteristics of the device stay unchanged.

By reducing the external applied magnetic field, the working frequency and periodic number of the electric field distribution are both reduced, the electron efficiency is a little bit low, but is acceptable. Therefore, we can change the working frequency and mode of the planar gyrotron by adjusting the guided magnetic field.

Next, we optimize the parameters of the planar gyrotron by using the particle simulation and genetic algorithms, which has been used to optimize the relativistic backward wave oscillator.[20]

References

[1] Siegel P H 2002 *IEEE Trans. Microwave Theory Technol.* **50** 910
[2] Booske J H, Dobbs R J, Joye C D, Kory C L, Neil G R, Park G, Park J and Temkin R J 2011 *IEEE Trans. Terahertz Sci. Technol.* **1** 54
[3] Zhang T Y and Cao J C 2004 *Chin. Phys.* **13** 1742
[4] Chen Z and Cao J C 2013 *Chin. Phys. B* **22** 059201
[5] Glyavin M Y, Luchinin A G and Golubiatnikov G Y 2008 *Phys. Rev. Lett.* **100** 015101
[6] Bratman V, Glyavin M, Idehara T, Kalynov Y, Luchinin A, Manuilov V, Mitsudo S, Ogawa I, Saito T, Tatematsu Y and Zapevalov V 2009 *IEEE Trans. Plasma Sci.* **37** 36
[7] Wang G, Wang J, Tong C, Li X, Wang X, Li S and Lu X 2013 *Phys. Plasmas* **20** 043105
[8] Carr G L, Martin M C, McKinney W R, Jordan K, Neil G R and Williams G P 2002 *Nature* **420** 153
[9] Gong Y, Yin H, Yue L, Lu Z, Wei Y, Feng J, Duan Z and Xu X 2011 *IEEE Trans. Plasma Sci.* **39** 847
[10] Ginzburg N S, Zotova I V, Sergeev A S, Zaslavsky V Y and Zheleznov I V 2012 *Phys. Rev. Lett.* **108** 105101
[11] Wang J, Chen Z, Wang Y, Zhang D, Liu C, Li Y, Wang H, Qiao H, Fu M and Yuan Y 2010 *Phys. Plasmas* **17** 073107
[12] Wang J, Wang Y and Zhang D 2006 *IEEE Trans. Plasma Sci.* **34** 681
[13] Wang J G 2013 *Mod. Appl. Phys.* **4** 251 (in Chinese)
[14] Wang J, Zhang D, Liu C, Li Y, Wang Y, Wang H, Qiao H and Li X 2009 *Phys. Plasmas* **16** 033108
[15] Zhang H, Wang J, Tong C, Li X and Wang G 2009 *Phys. Plasmas* **16** 123104
[16] Li X, Wang J, Song Z, Chen C, Sun J, Zhang X and Zhang Y 2012 *Phys. Plasmas* **19** 083111
[17] Wang G, Wang J, Li S, Wang X, Tong C and Lu X 2013 *Acta Phys. Sin.* **62** 150701 (in Chinese)
[18] Li S, Wang J, Tong C, Wang G, Lu X and Wang X 2013 *Acta Phys. Sin.* **62** 120703 (in Chinese)
[19] Li X Z, Wang J G, Sun J, Song Z M, Ye H, Zhang Y C, Zhang L J and Zhang L G 2013 *IEEE Trans. Electron Dev.* **60** 2931
[20] Chen Z, Wang J, Wang Y, Qiao H, Zhang D and Guo W 2013 *Phys. Plasmas* **20** 113103